Available online at www.sciencedirect.com
ScienceDirect
Trans. Nonferrous Met. Soc. China 25(2015) 3339−3347
Transactions of Nonferrous Metals Society of China
www.tnmsc.cn

Corrosion degradation behavior of Mg−Ca alloy with high Ca content in SBF

Yi-chi LIU[1], De-bao LIU[1], Yue ZHAO[1,2], Min-fang CHEN[1]

1. School of Materials Science and Engineering, Tianjin University of Technology, Tianjin 300384, China;
2. School of Mechanical, Materials and Mechatronic Engineering, Faculty of Engineering and Information Sciences, University of Wollongong, Northfield Ave, Wollongong, NSW 2522, Australia

Received 27 November 2014; accepted 25 March 2015

Abstract: The corrosion degradation behavior of a Mg−Ca alloy with high Ca content aiming for a potential bone repair material in the simulated body fluid (SBF) was investigated. The microstructure and phase constitution of the pristine Mg−30%Ca (mass fraction) alloy were characterized with scanning electron microscopy (SEM) and X-ray diffraction (XRD). The Mg−30%Ca alloy samples were immersed in the SBF for 90 d, and the morphology, composition and cytotoxicity of the final corrosion product were examined. It is found that Mg−30%Ca alloy is composed of α-Mg and Mg_2Ca phases. During the corrosion process in the SBF, the Mg_2Ca phase acts as an anode and the α-Mg phase acts as a cathode. The final corrosion product of the Mg−30%Ca alloy in SBF includes a small amount of black precipitates and white suspended particles. The white suspended particles are $Mg(OH)_2$ and the black particles are believed to have a core−shell structure. The cytotoxicity experiments indicate that these black precipitates do not induce toxicity to cells.

Key words: Mg−Ca alloy; corrosion behavior; corrosion product; cytotoxicity

1 Introduction

In recent years, the research on a new generation of Mg-based biodegradable alloys has attracted sharply increasing attention [1−3]. As a lightweight metal with mechanical properties similar to those of natural bone and in vivo degradability via corrosion in the electrolytic environment of the body, Mg and its alloys have the potential to be used in biocompatible, osteoconductive, degradable implants for load-bearing and bone repairing applications. At present, the major drawback of Mg alloys serving as implant materials is their high corrosion rate in physiological environment, and thereby the loss of their mechanical integrity before tissues could sufficiently heal [4−7]. The corrosion rate of Mg can be improved in various ways, mainly by surface coating and alloying [8−11].

Ca is one of the common alloying elements for Mg and plays a crucial role in the formation of bone [12,13]. The previous studies have shown that Mg−Ca alloys degrade within bones and have good biocompatibility both in vivo and in vitro [14,15]. However, systematic study on the corrosion degradation behavior of high Ca content Mg−Ca alloys is lacking in literature.

Recently, some researches have indicated that the Mg−Ca alloy was absorbed completely except for a small amount of non-biodegradable Mg particles [15,16]. For the pure Mg, MAKAR and KRUGER [17] also reported that residual Mg particles were locally formed by the dissolution of the surrounding matrix after 7 d immersion in sodium borate (pH=9.2), but its bio-security had not been assessed in the previous work. In this work, a Mg−30%Ca alloy, featured with large amount of intermetallic compound secondary phase, was studied to clarify the role of the secondary phase in the corrosion degradation process in simulated body fluid (SBF), and the bio-security of residual particles was assessed by cytotoxicity text.

2 Experimental

2.1 Preparation of Mg−30%Ca alloy

Pure Mg (99.9%) ingot was melted at 720 ºC under the protection of gas mixture containing SF_6 and N_2. The calculated amount of Mg−45%Ca (mass fraction) master alloy was added to the Mg melt and then held for 30 min to ensure that the Mg−Ca master alloy got melted and

Foundation item: Project (51271131) supported by the National Natural Science Foundation of China
Corresponding author: De-bao LIU; Tel: +86-22-60214008; E-mail: debaoliu@126.com
DOI: 10.1016/S1003-6326(15)63968-1

diffused sufficiently. After that, the Mg−30%Ca (mass fraction) alloy melt was cast into a steel mould at 670 °C.

2.2 Characterization

The miscrostructural observations were performed on an optical microscope (OLYMPUSU−TV0.5XC−3) and a scanning electron microscope (SEM, JOEL 6700F, Japan). The phase constitution was characterized by X-ray diffraction (XRD, Rigaku D/max/2500PC).

The SBF immersion test was carried out in accordance with ASTM−G31−72[18]. The pH value of the SBF was adjusted to 7.4, and the temperature was kept at 37 °C in a water bath. The ion concentration was tested using a multi-parameter ion analyzer (HANNA HI83200). Three tests were taken for each measurement. After different immersion periods, the samples were removed from SBF and then carefully rinsed with distilled water before they are dried by warm air. The corrosion products were then removed by a chromate solution for the surface morphology and composition characterization by SEM, energy dispersion spectroscopy (EDS), XRD and X-ray photoelectron spectroscopy (XPS).

The electrochemical impedance spectroscopy (EIS) experiments were performed in a three-electrode cell, using a Pt foil as the counter electrode and a Ag/AgCl (saturated KCl) electrode as the reference electrode, using a Zahner Zennium electrochemical workstation with the frequency range of 100 kHz to 1 mHz and the sinusoidal signal perturbation of 10 mV.

L-929 cells were cultured in the Dulbecco's modified Eagle's medium (DMEM), 10% (volume fraction) fetal bovine serum (FBS), 100 U/mL penicillin and 100 mg/mL streptomycin at 37 °C in a humidified atmosphere with 5% CO_2. The cytotoxicity tests were carried out by indirect contact. The extracts were prepared according to GB/T 16886 [19]. The corrosion products were sterilized by irradiation. The extraction medium was diluted to 50% and 10%, sequentially. The cells were incubated in 96-well flat-bottomed cell culture plates at 50 cell/μL medium in each well and incubated for 24 h to allow attachment. The medium was then replaced with 100 μL extracts. The cells was incubated in a humidified atmosphere with 5% CO_2 at 37 °C for 2, 4 and 7 d, respectively, and then the cell viability was measured by MTT (methyl thiazolyl diphenyl-tetrazolium bromide).

3 Results and discussion

3.1 Phase constitution and microstructures

Figure 1 shows the XRD pattern of the Mg−30%Ca alloy. In addition to the major Mg phase, the peaks of the Mg_2Ca phase were also detected. Figure 2 shows the microstructure and EDS results of Mg−30%Ca alloy sample. A eutectic lamellar structure can be seen at the grain boundaries. Figures 2(c) and (d) show the EDS analysis results of matrix phase and precipitate phase, respectively. The mole fractions of Ca are 2.38% in the matrix and 26.22% in the precipitate phase, and combined with the XRD result and Mg−Ca phase diagram, the matrix phase and precipitate phase are α-Mg and Mg_2Ca, respectively.

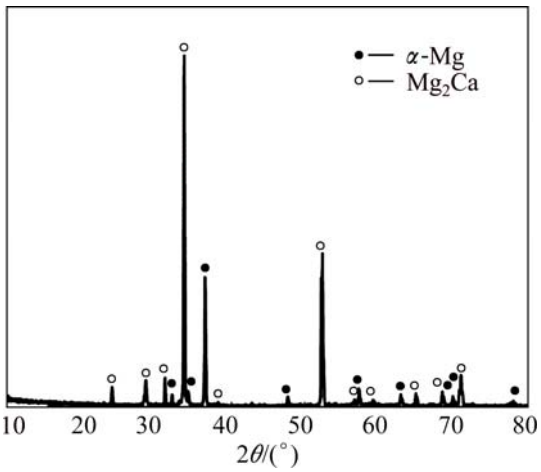

Fig. 1 XRD pattern of Mg−30%Ca alloy

3.2 Electrochemical behavior in SBF

Figure 3 shows the polarization curves of Mg−30%Ca alloy recorded in the SBF solutions at different testing time. It can be seen that the corrosion potential continuously decreases and the anodic polarization current density increases in the first 8 h immersion. The corrosion potential is the combined result of the electrochemical reaction at the interface between sample and the SBF solution. The corrosion potential decreases in the first 8 h immersion, indicating that the corrosion sensitivity increases with the extension of immersion time. However, in the period of 8−24 h immersion, the corrosion potential gradually increases and the anodic polarization current density decreases, which can be attributed to the passivation effect of corrosion products on the sample surface.

Figure 4 presents the EIS measurement results of the Mg−30%Ca alloy immersed in SBF solution for 4−24 h. The EIS spectrum is characterized by two capacitive semicircles and an inductive semicircle: a capacitive loop in the high frequency region, a capacitive loop in the middle frequency region, and an inductive loop in the low frequency region. It can be found that in the first period of 8 h immersion, the capacitive loop in the high frequency region continues to shrink, suggesting that the corrosion rate continues to increase in the initial stage of immersion. However, when the immersion time exceeds 8 h, the capacitive loop in the high frequency

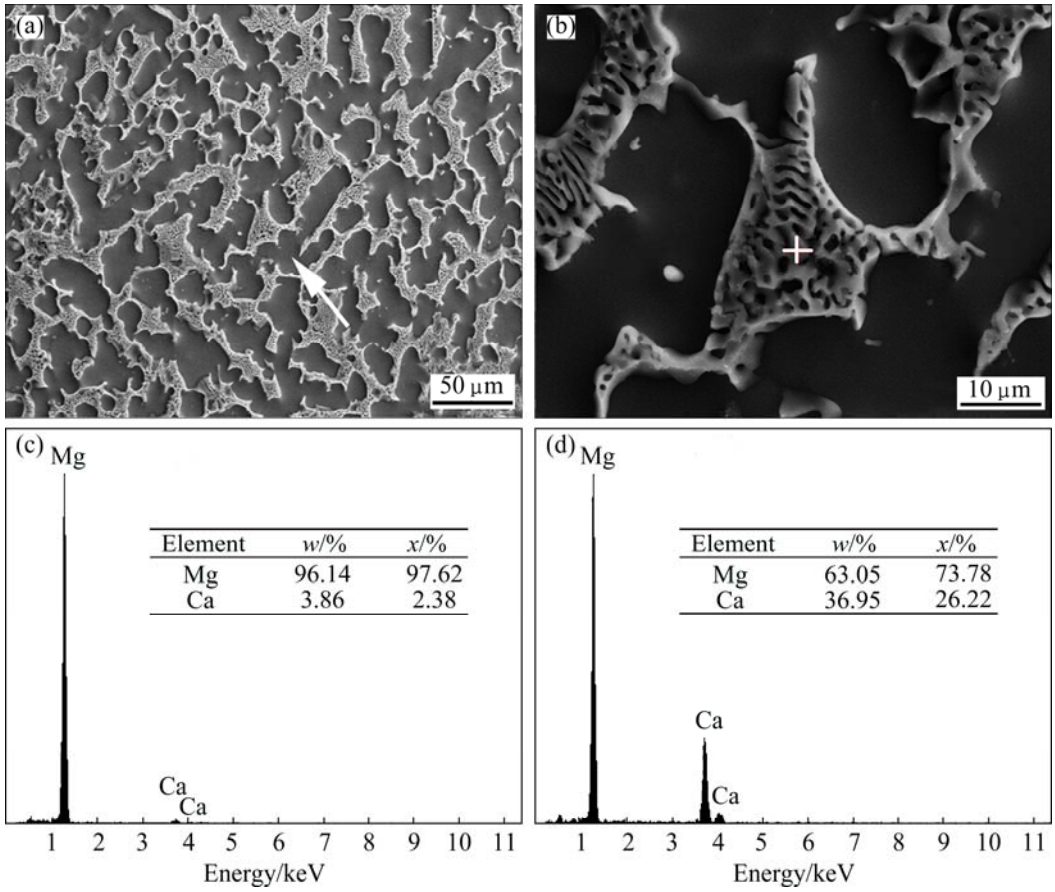

Fig. 2 SEM micrographs (a,b) of Mg−30%Ca alloys and EDS spectra of matrix phase (c) (marked by arrow in (a)) and precipitate phase (d) (marked by cross-hair in (b))

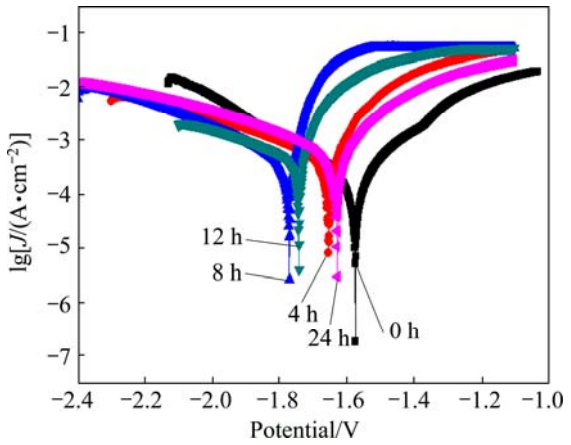

Fig. 3 Polarization curves recorded on Mg−30%Ca alloy electrodes at different immersion time

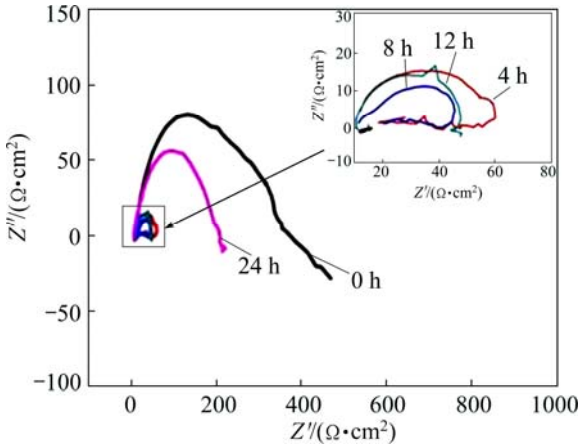

Fig. 4 Nyquist plots of Mg−30%Ca samples immersed in SBF with different time

region gradually expands until the immersion time reaches 24 h, suggesting that the corrosion rate continues to decrease. Once the Mg−30%Ca alloy surface contacts with the SBF solution, the electric double layer forms. The SBF solution contains a certain amount of chloride ions, which will penetrate the electric double layer and electrochemically react with the alloy matrix to cause pitting corrosion.

Therefore, the corrosion product layers formed in the first 8 h do not have sufficient protection effect against pitting corrosion. With increasing the immersion time, some infusibility corrosion products continually deposit on the sample surface, which have a protective effect and can inhibit pitting expansion, leading to fact that the high-frequency capacitive arc expands after a certain immersion time.

3.3 Immersion test of Mg−30%Ca alloy

Figure 5 shows the SEM image of the surface of Mg−30%Ca alloys immersed in SBF for 25 min. It can be clearly seen that crack is observed on the surface of sample. Therefore, the corrosion product layer does not have good protection effect for the matrix. The EDS analysis results (as shown in Fig. 5(b)) indicate that the corrosion layer is constituted by Ca, Mg and O. Since H cannot be measured by EDS, the existence of hydroxides cannot be ruled out. Figure 6 illustrates the XRD patterns of Mg−30%Ca alloy samples after immersing in SBF for different immersion periods. The XRD spectra show that $Mg(OH)_2$, MgO and $CaCO_3$ are the dominant corrosion products in the Mg−30%Ca alloy sample immersed in SBF for 25 min.

Figures 7(a) and (b) show the surface morphologies of Mg−30%Ca alloy samples after immersion in SBF for 15 and 25 min, respectively. After immersion for 15 min, pitting corrosion can be observed on the surface and increases significantly after immersion for 25 min. Figure 7(c) shows that the corrosion occurs at the grain boundary which enrichs with a large number of Mg_2Ca.

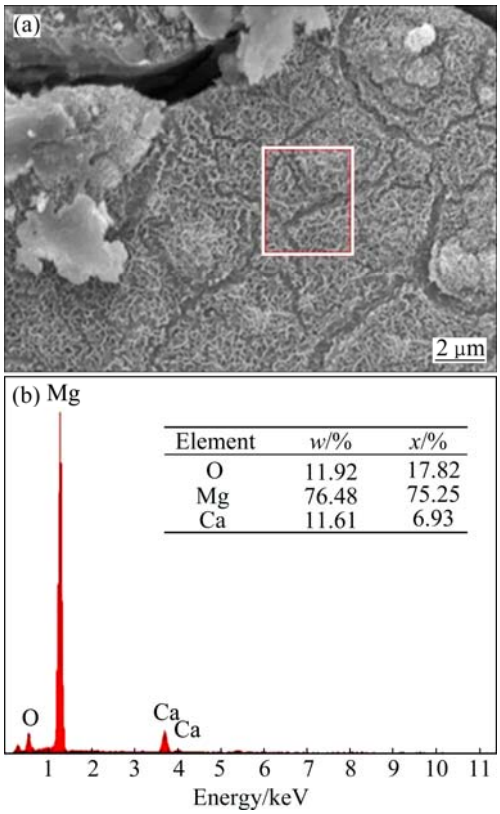

Fig. 5 SEM micrograph of Mg−30%Ca alloy after immersion in SBF for 25 min (a) and EDS spectrum corresponding to framed area in (a) (b)

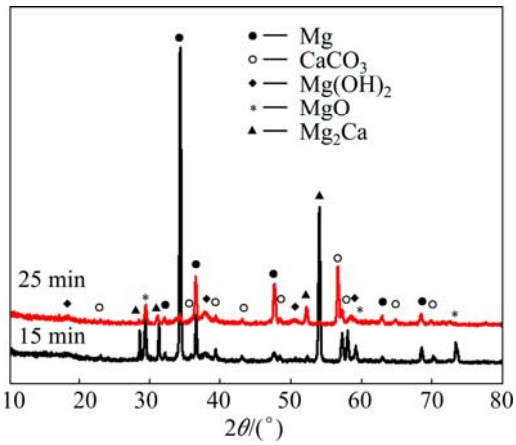

Fig. 6 XRD patterns of Mg−30%Ca alloys immersed in SBF for 15 min and 25 min

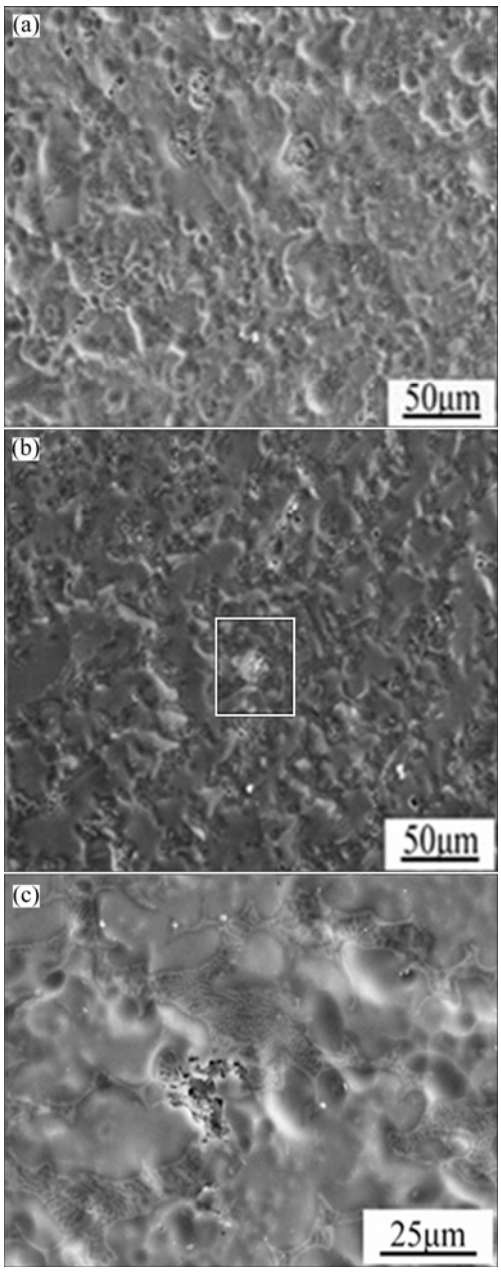

Fig. 7 SEM micrographs of Mg−30%Ca alloy after immersion for 15 min (a) and 25 min (b) and SEM micrograph of framed area in (b) (c)

It indicates that the Mg_2Ca phase is preferred for corrosion in the Mg/Mg_2Ca galvanic corrosion system. This result is consistent with the relevant result reported by DU et al [20].

Figure 8 shows the XPS spectra of Mg−30%Ca alloy that was immersed in SBF for 3 min. Figure 8(a) depicts the XPS spectrum of Ca 2p of sample, and the curve-fitting of spectrum using four peaks gives a reasonable match. Those peaks are located at 350.9 eV ($2p_{3/2}$) and 347.5 eV ($2p_{1/2}$), 346.7 eV ($2p_{3/2}$) and 351.8 eV ($2p_{1/2}$), which are assigned as CaO [21] and $Ca(OH)_2$ [22] peaks, respectively. Similarly, the XPS spectrum of Mg 1s is also given (Fig. 8(b)), two peaks fitted are located at 1304.35 eV (1s) and 1302.7 eV (1s), which correspond to the peaks of MgO [23] and $Mg(OH)_2$ [24], respectively. The results of XPS analysis indicate that the main components of corrosion film are oxide and hydroxide of Mg/Ca at the beginning of immersion.

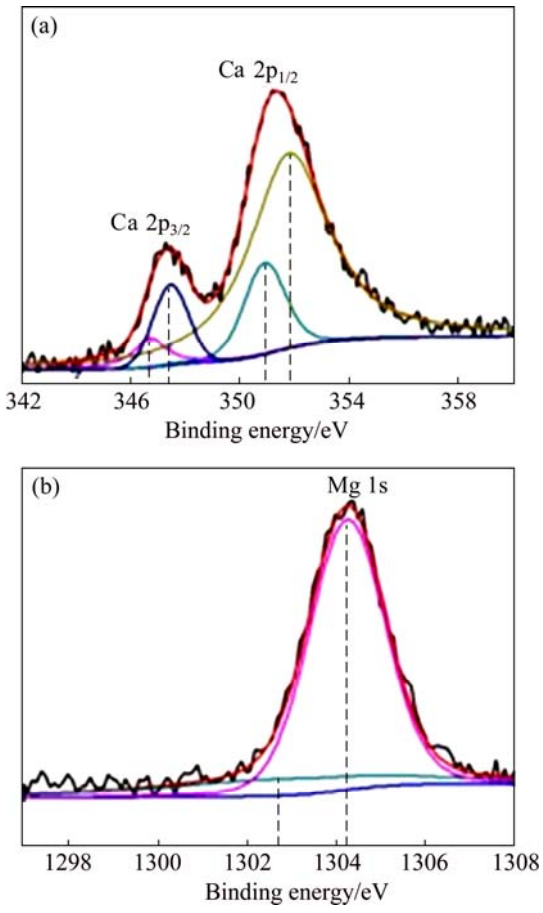

Fig. 8 XPS spectra of Ca 2p (a) and Mg 1 s (b) of Mg−30%Ca sample after immersion for 3 min

According to the above results, it is reasonable to believe that once the fresh Mg alloy surface is exposed to SBF, an oxide film (MgO/CaO) forms on the surface of Mg alloy immediately. The oxide film is not a stable presence in the SBF. Part of MgO converts to Mg $(OH)_2$ which is manipulated by a dissolution−precipitation mechanism [14]. The existence of chloride will maintain the homeostasis of this dissolution−precipitation process, i.e., $Mg(OH)_2$ reacts with chloride to form soluble $MgCl_2$. CaO is also a product extremely unstable in SBF. It will turn into $Ca(OH)_2$ and reacts with CO_3^{2-} to generate a small amount of precipitate on the surface. Since the underlying oxide film cannot prevent the diffusion of the electrolyte into the alloy surface, galvanic corrosion will occur. As mentioned above, the Mg phase is a cathode, and the Mg_2Ca phase is preferred for corrosion in the Mg/Mg_2Ca galvanic corrosion system.

Based on the above analyses, a corrosion model of Mg−Ca alloy was proposed, as shown in Fig. 9. An oxide film (MgO/CaO) immediately forms when the Mg−Ca alloy is immersed in SBF solution, which forms the innermost layer of the entire corrosion product layer (Fig. 9(a)). Then, the oxide grows into the hydroxide film by hydration reaction, which forms the intermediate corrosion production layer (Fig. 9(b)). Cl^- in SBF tends to convert hydroxide film into soluble chlorides which can diffuse into SBF solution from the alloy surface. Therefore, the electrolyte solutions readily penetrate to the alloy surface and the Mg/Mg_2Ca galvanic corrosion can be promoted. After a period of corrosion, some particles separate from the alloy surface when the Mg_2Ca phase at grain boundary is completely corroded. At the meantime, with increasing the concentrations of Mg^{2+} and Ca^{2+} ions, Mg/Ca salt, especially the carbonate, attaches to the matrix surface, leading to the fact that the corrosion rate drops significantly as they are nonconductive. Therefore, the outermost layer of entire corrosion product would be a mixture composed of Mg/Ca hydroxide and carbonate precipitate (Fig. 9(c)). In summary, the corrosion product film of Mg−Ca alloys is believed to have a multi-layered structure. The outermost layer is mainly a composite of $CaCO_3$/ $Mg(OH)_2$ precipitates, and the innermost layer is a dense mixture of MgO/CaO oxides, while the intermediate layer is composed of $Mg(OH)_2$.

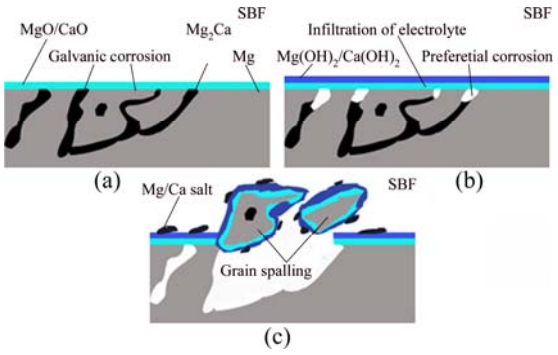

Fig. 9 Formation model of innermost layer (a), intermediate layer (b) and outermost layer (c) of entire corrosion product

3.4 Testing and analysis of corrosion products of Mg−Ca alloy in SBF

A small amount of black powder precipitates and white suspended particles are found in SBF solution after Mg−Ca alloy immersion for a period of time and the black powder is found very difficult to be further corroded even immersion in SBF exceeding 90 d. After centrifugal separation treatment, the mixture of black powder and suspended particles is obtained. Figure 10 presents the XRD patterns of this mixture powder and the single black powder. It can be seen that the main compositions of mixture powder are Mg, $Mg(OH)_2$, MgO and Mg_2Ca. Compared with the peak strength of $Mg(OH)_2$ of the black powder, that of the mixture powder increases obviously, indicating that the main composition of suspended particles should be $Mg(OH)_2$.

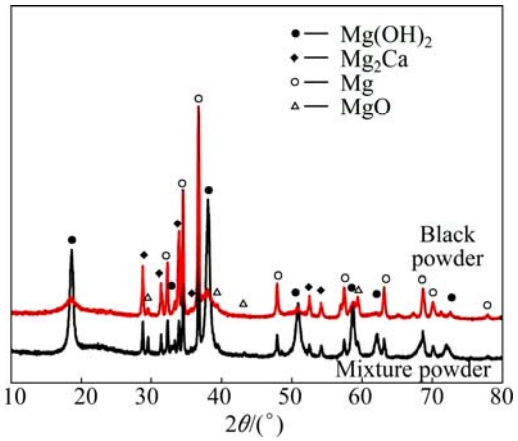

Fig. 10 XRD patterns of corrosion products

Figure 11(a) shows the morphology of black powder. It can be seen that these particles have irregular shape with a large amount of micro-particles deposited on it, as shown in Fig. 11(b). The EDS examination of the powder particles (Fig. 11(c)) indicates that the main components are Mg, Ca, O and C. This result is consistent with the XRD result of the powder particles. A profile picture given in Fig. 11(d) indicates a shell package around the Mg particle (indicated by arrow). Combining the EDS and XRD results of the powder particle, the typical schematic diagram of black powder particle is proposed in Fig. 11(d). The black powder should be a core−shell structure consisting of α-Mg particle core and $Mg(OH)_2$, MgO and Mg/Ca salt shell and this shell is very dense, therefore, these particles are very difficult to be further degraded in SBF.

3.5 Cytotoxicity text of corrosion products

The morphologies of L-929 cells cultured in the extraction media for a period of 2, 4 and 7 d, respectively, are presented in Fig. 12. All the results of the 100%, 50%, and 10% black corrosion product extraction media and the contrast group exhibit a healthy cell morphology with flattened spindle shape and adhered well. It can also be seen that the cell viability is positively influenced by

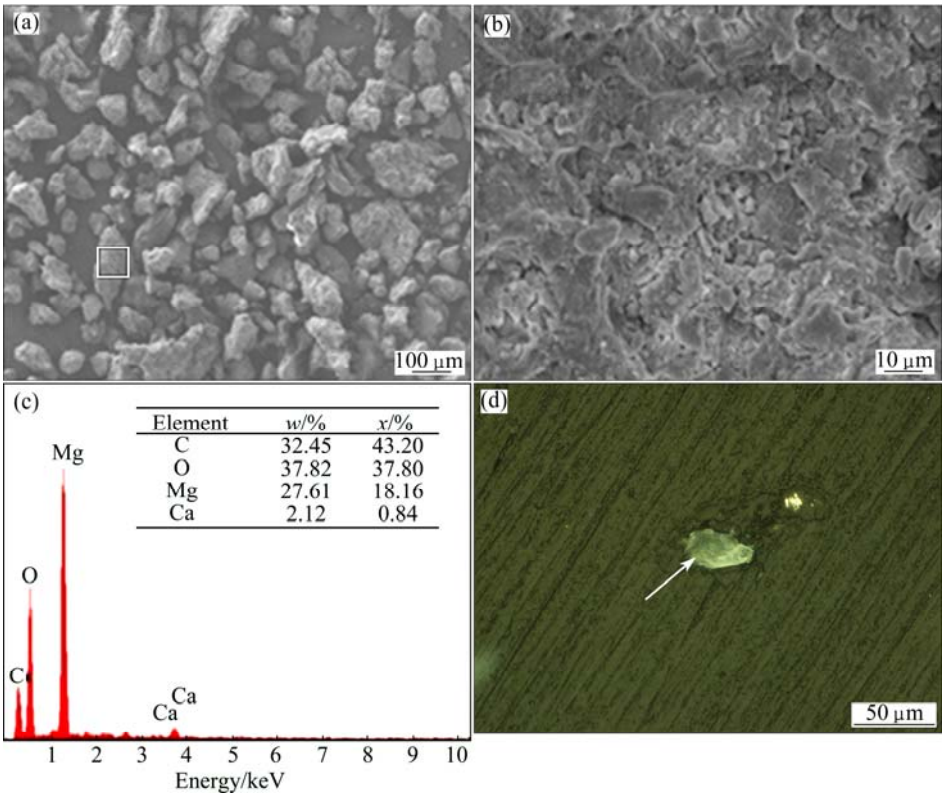

Fig. 11 SEM micrograph of black powder particles (a), SEM micrograph (b) and EDS spectrum (c) of particle of framed area in (a), and sectional view of black powder particle (d)

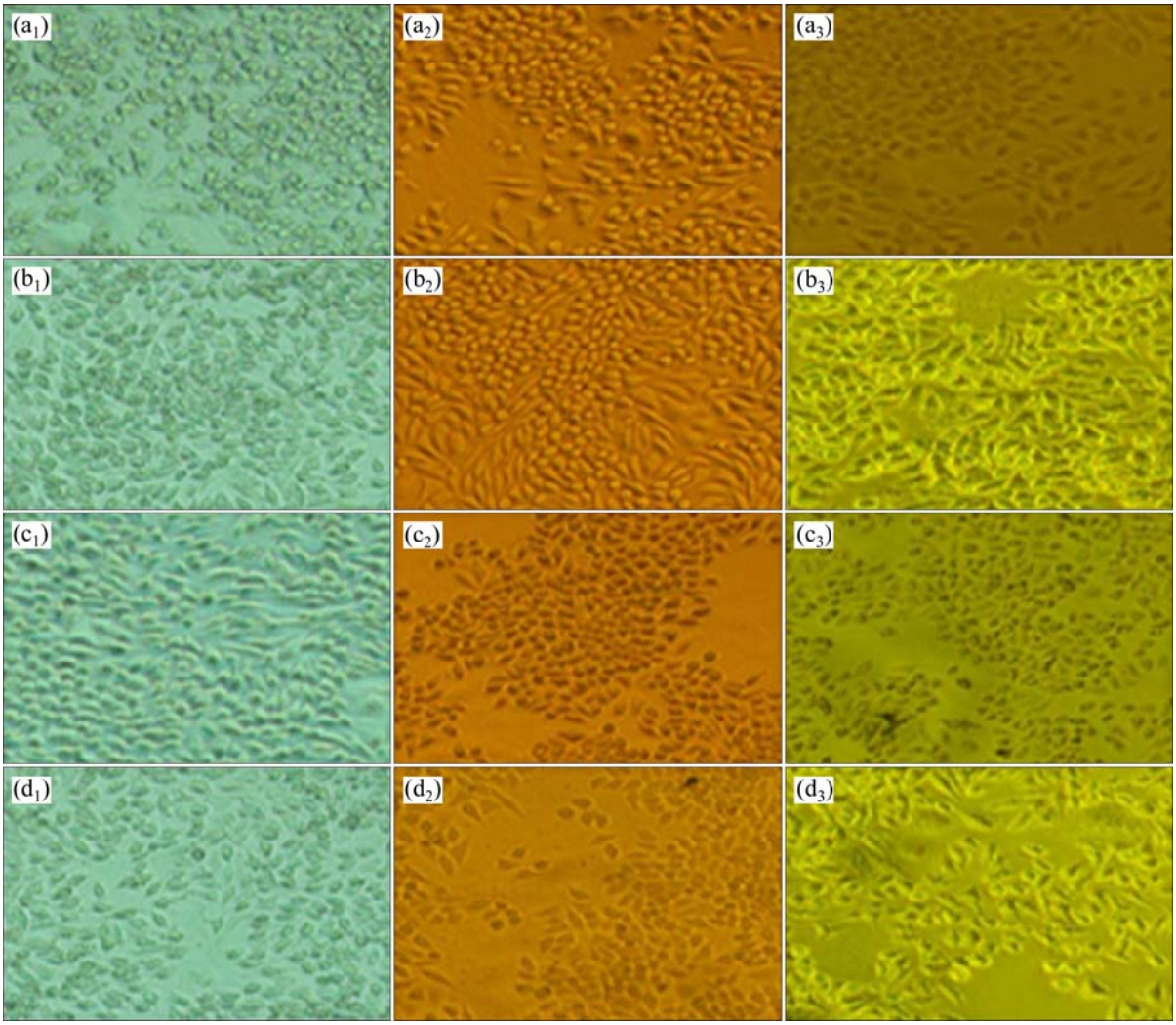

Fig. 12 Optical micrographs of L-929 cells cultured in contrast (a_1−a_3) and 100% extract (b_1−b_3), 50% extract (c_1−c_3), and 10% extract (d_1−d_3) for 2 d (a_1, b_1, c_1, d_1), 4 d (a_2, b_2, c_2, d_2) and 7 d (a_3, b_3, c_3, d_3)

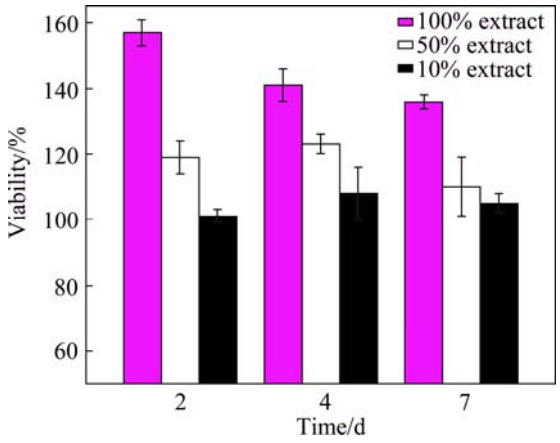

Fig. 13 L-929 cell viability cultured in different extracts after incubation for 2, 4 and 7 d

higher extract concentration (Fig. 13), suggesting that the Mg/Ca ions can effectively induce the growth of osteoblast cell.

As mentioned above, it is found that the black corrosion product is difficult to be further corroded under immersion in SBF for over 90 d. If the corrosion product residues in the human body, it may be swallowed by giant cell or macrophage. This is similar to the fact that the Ca salt produced in the corrosion process can be digested in the cell or absorbed by surrounding lymphoid tissue [25]. After the corrosion particles are phagocytosed by giant cell or macrophage, they can release a series of inflammatory factors such as interleukin IL-1β and IL-6. They can act on osteoclasts to lead to osteolysis. Mg−Ca alloys as bone fixation materials will produce corrosion particles in the degradation process, as reported by KIRKLAND et al [26]. Therefore, the biological safety of the corrosion product particles, which will remain in human body, is worthy to be further studied.

4 Conclusions

1) The Mg−30%Ca alloy is constituted by α-Mg and Mg_2Ca phases. During the process of corrosion, the Mg_2Ca phase acts as an anode and the α-Mg phase acts as a cathode.

2) The corrosion product film on the surface of Mg−30%Ca alloy in SBF is mainly constituted by $Mg(OH)_2$, MgO, CaO and $Ca(OH)_2$.

3) The corrosion product of the Mg−30%Ca alloy in SBF consists of a small amount of black powder precipitates and some white suspended particles. The white suspended particles are detected to be $Mg(OH)_2$ and the black particles are believed to have a core−shell structure consisting of α-Mg particle core and a dense salt shell of $Mg(OH)_2$, MgO and Mg/Ca mixture. The cytotoxicity experiments indicate that these black powder precipitates do not induce toxicity to cells.

References

[1] KANNAN M B, RAMAN R K. In vitro degradation and mechanical integrity of calcium-containing magnesium alloys in modified-simulated body fluid [J]. Biomaterials, 2008, 29(15): 2306−2314.

[2] STAIGER M P, PIETAK A M, HUADMAI J, DIAS G. Magnesium and its alloys as orthopedic biomaterials: A review [J]. Biomaterials, 2006, 27(9): 1728−1734.

[3] CHEN Y J, WANG Q D, LIN J B, LIU M P, HJELEN J, ROVEN H J. Grain refinement of magnesium alloys processed by severe plastic deformation [J]. Transactions of Nonferrous Metals Society of China, 2014, 24(12): 3747−3754.

[4] QI F, ZHANG D, ZHANG X, XU X. Effect of Sn addition on the microstructure and mechanical properties of Mg−6Zn−1Mn (wt.%) alloy [J]. Journal of Alloys and Compounds, 2014, 585: 656−666.

[5] WITTE F, HORT N, VOGT C, COHEN S, KAINER K U, WILLUMEIT R, FEYERABEND F. Degradable biomaterials based on magnesium corrosion [J]. Current Opinion in Solid State and Materials Science, 2008, 12(5): 63−72.

[6] DU Xiao-qing, YANG Qing-song, CHEN Yu, YANG Yang, ZHANG Zhao. Galvanic corrosion behavior of copper/titanium galvanic couple in artificial seawater [J]. Transactions of Nonferrous Metals Society of China, 2014, 24(2): 570−581.

[7] BAKHSHESHI-RAD H R, HAMZAH E, DAROONPARVAR M, YAJID M A M, KASIRI-ASGARANI M, ABDUL-KADIR M R, MEDRAJ M. In-vitro degradation behavior of Mg alloy coated by fluorine doped hydroxyapatite and calcium deficient hydroxyapatite [J]. Transactions of Nonferrous Metals Society of China, 2014, 24(8): 2516−2528.

[8] ZHENG Y F, GU X N, WITTE F. Biodegradable metals [J]. Materials Science and Engineering R: Reports, 2014, 77: 1−34.

[9] HORNBERGER H, VIRTANEN S, BOCCACCINI A R. Biomedical coatings on magnesium alloys—A review [J]. Acta Biomaterialia, 2012, 8(7): 2442−2455.

[10] CHU Cheng-lin, HAN Xiao, BAI Jing, XUE Feng, CHU Paul-kao. Surface modification of biomedical magnesium alloy wires by micro-arc oxidation [J]. Transactions of Nonferrous Metals Society of China, 2014, 24(4): 1058−1064.

[11] CHEN Bin, WANG Ri-chu, PENG Chao-qun, FENG Yan, WANG Nai-guang. Influence of Al−Mn master alloys on microstructures and electrochemical properties of Mg−Al−Pb−Mn alloys [J]. Transactions of Nonferrous Metals Society of China, 2014, 24(2): 423−430.

[12] SHADANBAZ S, DIAS G J. Calcium phosphate coatings on magnesium alloys for biomedical applications: A review [J]. Acta Biomaterialia, 2012, 8(1): 20−30.

[13] ILICH J Z, KERSTETTER J E. Nutrition in bone health revisited: A story beyond calcium [J]. Journal of the American College of Nutrition, 2000, 19(6): 715−737.

[14] LI Z, GU X, LOU S, ZHENG Y. The development of binary Mg–Ca alloys for use as biodegradable materials within bone [J]. Biomaterials, 2008, 29(10): 1329−1344.

[15] GU X, ZHENG Y, CHENG Y, ZHONG S, XI T. In vitro corrosion and biocompatibility of binary magnesium alloys [J]. Biomaterials, 2009, 30(4): 484−498.

[16] PARK R S, KIM Y K, LEE S J, JANG Y S, PARK I I, YUN Y H, LEE M H. Corrosion behavior and cytotoxicity of Mg–35Zn−3Ca alloy for surface modified biodegradable implant material [J]. Journal of Biomedical Materials Research Part B: Applied Biomaterials, 2012, 100(4): 911−923.

[17] MAKAR G L, KRUGER J. Corrosion studies of rapidly solidified magnesium alloys [J]. Journal of the Electrochemical Society, 1990, 137(2): 414−421.

[18] ASTM G31−72 (1999). Standard practice for laboratory immersion corrosion testing of metals [S].

[19] GB/T 16886.1−2011. Biological evaluation of medical devices—Part 1: Evaluation and testing within a risk-management process [S].

[20] DU H, WEI Z, LIU X, ZHANG E. Effects of Zn on the microstructure, mechanical property and bio-corrosion property of Mg−3Ca alloys for biomedical application [J]. Materials Chemistry and Physics, 2011, 125(3): 568−575.

[21] XU J L, KHOR K A. Chemical analysis of silica doped hydroxyapatite biomaterials consolidated by a spark plasma sintering method [J]. Journal of Inorganic Biochemistry, 2007, 101(2): 187−195.

[22] KOLEVA D, van BREUGEL K, de WIT J H W, BOSHKOV N, FRAAIJ A L A. Composition and morphology of product layers in the steel/cement paste interface in conditions of corrosion and cathodic protection in reinforced concrete [J]. Electrochemical Society Transactions, 2007, 2(9): 127−139.

[23] SUN D M, SUN Z Q, LI A X, XU Z Y. Oxidation behaviour of MgF_2 in Ag−MgF_2 cermet [J]. Vacuum, 1999, 55(1): 39−44.

[24] LIU C, XIN Y, TIAN X, CHU P K. Corrosion behavior of AZ91 magnesium alloy treated by plasma immersion ion implantation and deposition in artificial physiological fluids [J]. Thin Solid Films, 2007, 516(2): 422−427.

[25] LIU C, XIN Y, TIAN X, CHU P K. The biodegradation mechanism of calcium phosphate biomaterials in bone [J]. Journal of Biomedical Materials Research, 2002, 63(4): 408−412.

[26] KIRKLAND N T, LESPAGNOL J, BIRBILIS N, STAIGER M P. A survey of bio-corrosion rates of magnesium alloys [J]. Corrosion Science, 2010, 52(2): 287−291.

高 Ca 含量 Mg−Ca 合金在模拟体液中的腐蚀降解行为

刘一驰[1]，刘德宝[1]，赵 越[1,2]，陈民芳[1]

1. 天津理工大学 材料科学与工程学院，天津 300384；
2. School of Mechanical, Materials and Mechatronic Engineering, Faculty of Engineering and Information Sciences, University of Wollongong, Northfield Ave, Wollongong, NSW 2522, Australia

摘 要：研究高 Ca 含量 Mg−Ca 合金作为骨修复材料在模拟体液中的腐蚀降解行为。采用扫描电子显微镜(SEM)和 X 射线衍射(XRD)对 Mg−30%Ca(质量分数)合金的显微组织及相成分进行表征。将 Mg−30%Ca 合金在模拟体液中浸泡 90 d 后，观察和测试最终产物的微观形貌、成分以及细胞毒性。结果表明：Mg−30%Ca 合金的主要相成分为 α-Mg 和 Mg_2Ca 相，在浸泡过程中，Mg_2Ca 相作为阳极，而 α-Mg 相作为阴极；Mg−30%Ca 合金在模拟体液中浸泡的最终腐蚀产物由少量的的黑色沉淀颗粒和白色悬浮颗粒组成，白色悬浮颗粒为 $Mg(OH)_2$，而黑色沉淀颗粒具有核壳结构；细胞毒性实验证明黑色沉淀颗粒无细胞毒性。

关键词：Mg−Ca 合金；腐蚀行为；腐蚀产物；细胞毒性

(Edited by Mu-lan QIN)